frontiers in Energy Research

MINI REVIEW
published: 05 April 2021
doi: 10.3389/fenrg.2021.620203

A Mini-Review: Pyridyl-Based Coordination Polymers for Energy Efficient Electrochromic Application

Shiyou Liu[1], Ping Zhang[1], Jianjian Fu[1,2], Congyuan Wei[1] and Guofa Cai[1]**

[1]*Key Laboratory for Special Functional Materials of Ministry of Education, National & Local Joint Engineering Research Center for High-efficiency Display and Lighting Technology, School of Materials Science and Engineering and Collaborative Innovation Center of Nano Functional Materials and Applications, Henan University, Kaifeng, China,* [2]*School of Chemical and Environmental Engineering, Anyang Institute of Technology, Anyang, China*

Electrochromic devices (ECDs) have a broad range of application prospects in many important energy efficient optoelectronic fields, such as smart windows, anti-glare rearview mirrors, low-energy displays, and infrared camouflage. However, there are some factors restricting their development, such as low coloration efficiency, slow switching speed, and poor cycling stability. Coordination polymer (CP) is a promising active material for the fabrication of high-performance ECD because of its ultrahigh coloration efficiency, fast switching speed, and excellent cycling stability. In this review, current advances of CP in energy efficient ECDs are comprehensively summarized and evaluated. Specifically, the effects of composition, coordination bonding, and microstructure of the bipyridine- and terpyridine-based CP on EC performances are introduced and discussed in detail. Then, the challenges and prospects of this booming field are proposed. Finally, the broad application prospects of the CPs-based EC materials and the corresponding devices are also demonstrated, which hold numerous revolutionary effects over our daily life. Hopefully, this review would provide useful guidance and further promote progress on the electrochromic and other optoelectronic fields.

Keywords: Smart window, electrochromism, display, multicolor, coordination polymers

OPEN ACCESS

Edited by:
Shi Hu,
Tianjin University, China

Reviewed by:
Huan Pang,
Yangzhou University, China
Jijeesh Ravi Nair,
Politecnico di Torino, Italy

****Correspondence:***
Congyuan Wei
weicongyuan@henu.edu.cn
Guofa Cai
caiguofa@henu.edu.cn

Specialty section:
This article was submitted to Electrochemical Energy Conversion and Storage, a section of the journal Frontiers in Energy Research

Received: *22 October 2020*
Accepted: *08 February 2021*
Published: *05 April 2021*

Citation:
Liu S, Zhang P, Fu J, Wei C and Cai G (2021) A Mini-Review: Pyridyl-Based Coordination Polymers for Energy Efficient Electrochromic Application. Front. Energy Res. 9:620203. doi: 10.3389/fenrg.2021.620203

INTRODUCTION

The environment is facing unprecedented challenges owing to a serious energy crisis and environmental pollution (Li M. et al., 2019; Huang et al., 2020; Xu et al., 2020). As one of the most promising strategies to guarantee the sustainable development of the social economy and environment, energy-saving has been receiving ever-increasing attention (Li et al., 2018; Zhang T. et al., 2020). Electrochromism, an important energy-saving technology, has been extensively investigated in both industry and academia (Cai et al., 2017; Cai et al., 2020; Ninomiya et al., 2020). In 1969, the electrochromic (EC) phenomenon of tungsten trioxide (WO_3) was first reported by Deb S. K. *et al.* The color of the WO_3 film can be reversibly changed from colorless to blue under the stimulation of negative voltage. Furthermore, electrochromic devices (ECDs) based on WO_3 film was first fabricated, which is considered as the origin of EC investigation (Deb, 2006). Typically, ECD includes an EC layer, an ion storage layer, and an ion conducting (electrolyte) layer, as well as two transparent electrodes. The EC layer is the key active component of the device which determines the EC performance. The ion storage layer, also known as the counter layer, can be used to balance the carriers transferred from the active EC layer, which can penetrate the electrolyte within configuration

of the ECD. Most ion storage materials, such as nickel oxide (Wang et al., 2019a), and Prussian blue (Lang et al., 2019), also exhibit superior EC performances. The electrolyte layer has ionic conducting and adhesive functions and can be used as the separator between the EC layer and ion storage layer, which has been regarded as one of the most influential factors for the ECD performances. More importantly, electrodes used in ECDs should simultaneously possess high electrical conductivity, high transparency, excellent thermal stability, good chemical durability, and suitable compatibility with other functional layers. On the basis of sophisticated comprehension about the ECD, some high-performance ECDs are being constructed, including smart eyewear glasses (Wang et al., 2019a), electronic paper (Lang et al., 2019), electronic displays (Wang et al., 2019b; Zhang et al., 2019), and wearable electronics (Keum et al., 2020). In particular, viologen-based ECD has recently been used in a Boeing 787 Dreamliner.

EC materials, as the core layer of ECDs, have achieved great progress in the past fifty years (Fan et al., 2015; Zhou et al., 2020). EC materials are mainly divided into two categories: inorganic and organic EC materials. Inorganic EC materials include transition metal oxides consisting of tungsten trioxide, nickel oxide, and so on (Cai et al., 2014; Tian et al., 2014). Although inorganic EC materials have made great progress in practical applications, the factors including slow switching speed, low coloration efficiency, and poor cycling stability still limit their commercialization. In recent years, organic materials have received more and more attention because of their numerous advantages such as high electronic conductivity, ample color variation, tunable compositions and structures, as well as the facilitation of large area solution-processing. Organic EC materials include small molecules, conjugated conducting polymers, and coordination polymers (CPs). Representative organic materials are viologen, polyaniline, poly (3,4-ethylenedioxythiophene): poly (styrene sulfonate) (PEDOT: PSS) and pyridyl-based CPs (Cai et al., 2013; Savagian et al., 2018; Christiansen et al., 2019; Feng et al., 2020). Among all these organic polymers, CPs can be self-assembled by coordination bonds between organic ligands and metal ions or clusters. CPs have drawn more attention because of their significant merits, including their fascinating properties in chemistry, physics, optoelectronics, and so on.

Compared with inorganic metal oxide EC materials, the raw materials for preparing organic electrochromic materials are extensive and widely available, such as pyridine-based and thiophene-based derivatives. The organic precursor (ligand) of CPs could be purified by means of sublimation, recrystallization, chromatographic column, and so on, to improve the yield and quality of the final products. Hence, high-quality CPs would be acquired. A lot of CPs could be achieved by modulating the organic ligand or metal ion, and further tuning the final EC performances. This will provide plenty of materials used in different daily life scenarios (Takada et al., 2015). On the other hand, for inorganic EC materials, sputtering and vacuum evaporation are usually used to deposit thin film, which is expensive and energy-consuming. In contrast, organic EC films can be fabricated by spin coating, electro-polymerization, and inject printing, facilitating large scale preparation and commercialization (Somani and Radhakrishnan, 2002).

Electrochromism refers to materials or devices whose optical properties can be reversibly and steadily changed under an alternating electric field (Wałęsa-Chorab et al., 2017). Therefore, electrochemical and spectroscopy-related technologies are frequently used to comprehensively evaluate the performances of EC materials and devices (Cai et al., 2016a). Generally, the performances of EC materials are often characterized via photoelectrochemical measurements in the form of thin film or device (Zhang et al., 2019). Particularly, the main parameters to evaluate the EC materials or devices include optical modulation, switching speed, coloration efficiency, cycling stability, and optical memory.

First, optical modulation is defined as the optical properties difference between colored state and bleached state, and it represents the light modulation ability. The largest optical modulation is 100%; in other words, the materials or devices can be reversibly converted between two states: complete transparency and full opaque (Cai et al., 2016b). Second, switching speed is defined as the time required to reach 90% of the optical modulation. At present, the recognized EC mechanism is the ion and electron injection/extraction process into/from the active EC materials. Therefore, the faster ions and electrons transfer, the faster the switching speed. Generally, the EC materials with an ultrafast switching speed (millisecond class at least) are suitable for scenes that require fast color switching, such as energy efficient displays, car's rearview mirrors, electronic books, smart eyewear glasses, and so on. Third, coloration efficiency can comprehensively reflect the quality of EC materials. It can be defined as the change of optical density (ΔOD) at certain wavelengths (λ) caused by the amount of charge (ΔQ) embedded per unit area of the EC film. We can calculate the coloration efficiency (CE) with the following formula:

$$\Delta \mathrm{OD}(\lambda) = \log\left(\frac{T_b}{T_c}\right), \tag{1}$$

$$\mathrm{CE}(\lambda) = \frac{\Delta \mathrm{OD}(\lambda)}{\Delta Q}, \tag{2}$$

where T_b and T_c represent transmittance in bleached and colored states, respectively. Usually, the high value of coloration efficiency means that the EC material or device shows large optical modulation with low energy consumption. Last, cycling stability is an important parameter to estimate whether an ECD can be commercialized. Generally, it can be evaluated by comparing the EC performance after thousands or even tens of thousands of electrochemical cycles. Ultimately, optical memory is the ability of an ECD to maintain its optical properties in a colored or bleached state after voltage-off, which is also called bistability. In a word, excellent EC materials should possess large optical modulation, fast color switching speed, high coloration efficiency, and long-term optical memory.

Although a few excellent reviews have been published about the development of organic EC materials in the optoelectronic

field, most primarily focus on traditional conducting polymers or organic small molecules (Lahav and van der Boom, 2018; Yen and Liou, 2018; Wang et al., 2019c). For example, Hung et al. introduced synthetic approaches to triphenylamine-based polymers and their potential applications (Yen and Liou, 2018). Ho and co-workers summarized recent advances of viologen-based derivatives and their corresponding ECD performances (Madasamy et al., 2019). Mei et al. discussed the material development of each functional layer and the reasonable design as well as fabrication strategies for high-performance ECDs (Li X. et al., 2019). However, few reviews focus on the development of pyridine-based CPs EC materials. Herein, this review comprehensively summarizes the latest developments of pyridyl-based CPs in the EC field. The effect of the bond, order, and structure of the ligand on the properties of EC materials are discussed in detail. In addition, it also introduces the construction methods and principle of multicolor EC materials. Then, the effect of different film coating methods on the EC performance is summarized. Finally, the challenges and prospects for further development of CPs in this booming field are outlined. We further provide an outlook concerning trends and issues in this field. We hope that this review will provide fundamental theoretical guidance for the design of EC materials or devices with better performance in the future.

SYNTHESIS, MECHANISM, STRUCTURE OF COORDINATION POLYMERS, AND FUNCTIONALIZED DEVICES

Synthesis of Coordination Polymers for EC Application

An advantage of CPs is that their structures and properties can be tunable through rational design and component selection (Kung et al., 2013; Duan et al., 2019). Because of these exciting properties and flexibility in molecular-level structural design, CPs are considered as one of the most promising candidates in EC materials (Cai et al., 2020a; Mondal et al., 2020a; Zhang J. et al., 2020).

The Synthetic Methods

There are many methods to synthesize CPs, such as solvothermal (Rubio-Gimenez et al., 2018), liquid-liquid interfacial synthesis (Takada et al., 2015), and reflux under inert atmosphere (Bera et al., 2020). Among them, liquid-liquid interfacial synthesis and reflux are widely used. Liquid-liquid interfacial synthesis is a method in which the ligand and the metal ion complexed at the interface of the two liquid phases in an orderly manner. The unique design principle of this liquid-liquid interfacial synthesis method can enable the formation of a long-range ordered microstructure and homogeneous interface properties (Dey et al., 2017). Another commonly used method is reflux of the mixed solution of ligand and metal ion under an inert gases atmosphere. This facile method can control the degree of polymerization during the reaction process. The representative synthetic methods of CPs are shown in **Scheme 1**.

The Naming Rule of Coordination Polymers

Because the metal ions possess positive charges, CPs synthesized by complexation ligands with metal ions are polycations (Leem et al., 2015). To maintain electrical neutrality, the counter anions will surround the area nearby the polymer skeleton. Therefore, a complete CP unit consists of metal ions, counter anions, and ligands; each of them may affect the EC performance. In addition, the ligands widely used in EC fields are listed and numbered to rename the subsequent CPs conveniently (**Figure 1**). The naming rules are as follows:

$$M - \mathrm{CP}(X) - N,$$

where M is metal ion that is involved in coordination, X corresponds to the numbered ligand as shown in **Figure 1**, and N refers to the counter anions. Therefore, Fe-CP(1)-OAc represents the CP produced by the coordination between ferrous acetate and ligand 1 (**Figure 1**).

Electrochromic Mechanism

CPs often display metal center electronic transitions including d-d* transitions (transition metal-based CPs) and d-f* transitions (lanthanide metal-based CPs). In addition, both metal-to-ligand charge transfer (MLCT) and ligand-to-metal charge transfer

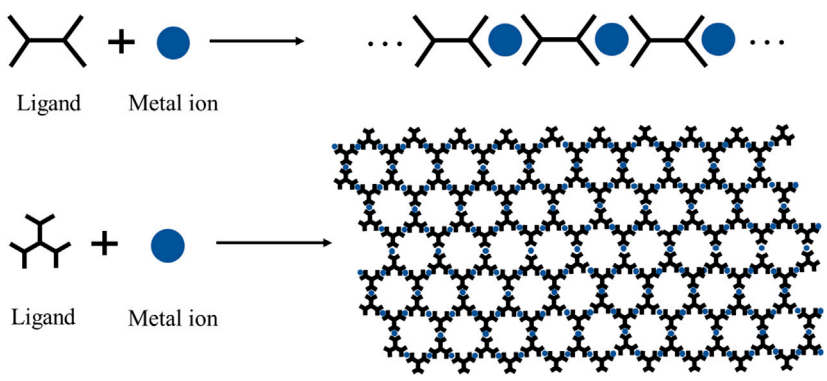

SCHEME 1 | The representative synthetic diagrams of CPs.

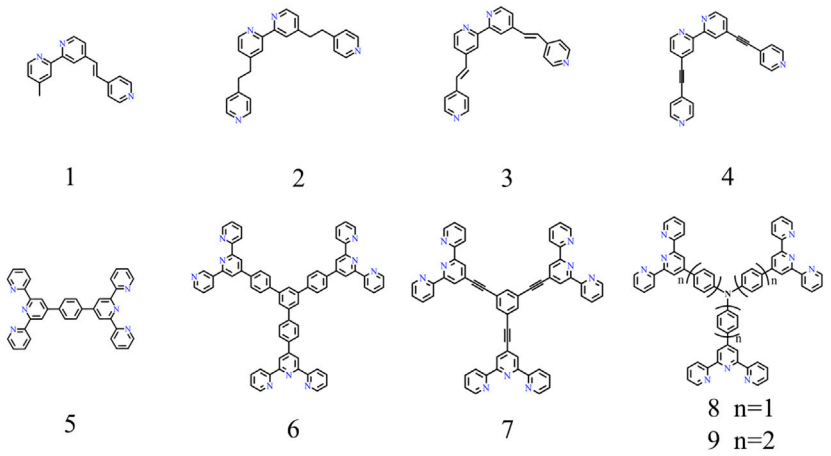

FIGURE 1 | Bipyridine-based (the first row) and terpyridine-based (the second row) ligands for EC field.

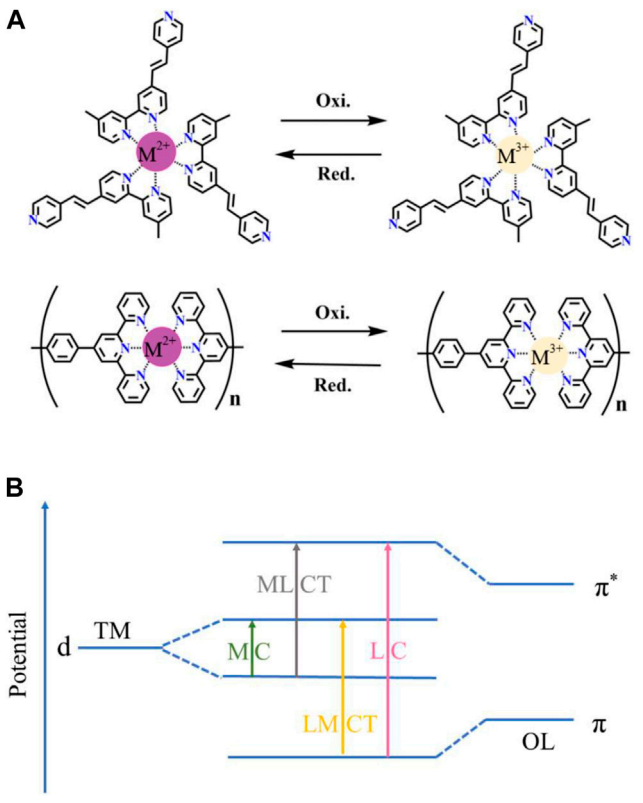

FIGURE 2 | (A) EC mechanism of bipyridine-based CPs (the first row) and terpyridine-based CPs (the second row) (M: Metal ion). **(B)** The possible electronic transitions in CPs (MC: metal center, LC: ligand center, TM: transition metal, OL: organic ligand).

(LMCT) absorption usually exist in CPs. The MLCT refers to the charge transfer process from the d orbital of the metal to the π* orbital of the organic ligand within the CPs molecule, while the LMCT denotes the charge transfer from the π orbital of the organic ligand to the d* orbital of the metal (Higuchi, 2014). The color of the CP can be changed reversibly with the redox reaction of the M^{2+}/M^{3+} couple under the applied alternating potential (**Figure 2A**); this phenomenon is called electrochromism. However, it should be noted that the CP-8 exhibits distinct multicolor EC performances because both parts of triphenylamine and [M(terpyridyl)$_2$] possess unique EC properties. The possible electronic transitions of most CPs corresponding to the EC process are summarized in **Figure 2B**.

The Effect of Structure on Electrochromic Performance

The Effect of Structure on Initial Color and Solubility

To date, the typical ligands used to synthesize EC materials are bipyridine-based (L1-L4 in **Figure 1**) and terpyridine-based ligands (L5-L9 in **Figure 1**). Numerous studies have been conducted to investigate the effects of metal ions, counter anions, and ligands on EC performances. The initial color of a CP can be adjustable by changing the metal species or modifying the organic ligands. According to this assumption, a CP with the same ligand but different metal ions (Fe^{2+}, Co^{2+}, Ru^{2+}, Os^{2+}) shows different colors. For example, red-, pink-, orange-, and blue-color was obtained in the corresponding CP(5) based on Ru(II) (Muronoi et al., 2013), Os(II) (Bera et al., 2019), Co(II) (Hsu et al., 2016), and Fe(II) (Hu et al., 2013), respectively. Similarly, the CP with different ligands complex with the same ion (II) also presents different colors. For instance, the sample synthesized by complexation 1,3,5-tris(1,10-phenanthrolyl) benzene (L1) (Mondal et al., 2020b) and different bond order pyridine-bipyridine ligands (H_2C-CH_2(L2), HC = CH(L3), C≡C (L4)) with the same iron (II) can achieve bluish gray, pinkish, gray, and red color, respectively (Shankar et al., 2015). In addition, the source of ion (II) does not influence the initial color of CPs, but affects the materials solubility and EC performances. As a typical CP material, Fe-CP(5) exhibits an outstanding EC performance. Hence, we choose the representative Fe-CP(5) as an example to elaborate on the effect of counter anions on its solubility in the following part.

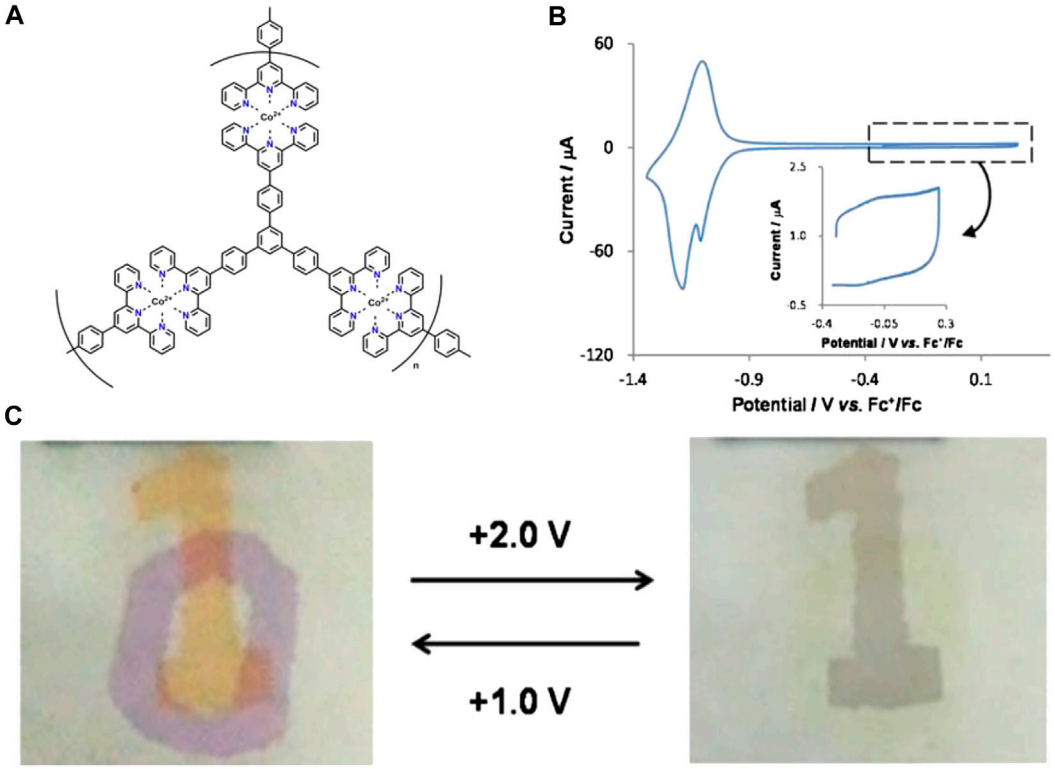

FIGURE 3 | (A) Structure of Co-CP(6)-BF4 **(B)** CV of Co-CP(6)-BF4 on ITO substrate in 1 M Bu4NClO4-CH2Cl2 solution. **(C)** Operation of the dual EC device with Fe-CP(6)-BF4 and Co-CP(6)-BF4. Adapted with permission (Zhang J. et al., 2020). Copyright 2015, American Chemical Society.

For example, the Fe-CP(5)-Cl, Fe-CP(5)-BF_4 and Fe-CP(5)-PF_6 can be respectively obtained by complexation of $FeCl_2$, $Fe(BF_4)_2$, or $Fe(PF_6)_2$ with L5. Fe-CP(5)-Cl and Fe-CP(5)-BF_4 are both insoluble in methanol (MeOH) and CH_3CN. Nevertheless, Fe-CP(5)-PF_6 is insoluble in MeOH but soluble in CH_3CN. On the contrary, Fe-CP(5)-OAc is soluble in MeOH but not CH_3CN (Bera et al., 2020). It is convenient to prepare the EC film by spraying the EC materials on the substrate, as the EC materials can be dissolved in a low-boiling solvent (such as methanol or ethanol). Meanwhile, since Fe-CP(5)-OAc is insoluble in CH_3CN, this could enable it to act as the EC layer in the ECD which CH_3CN is an electrolyte component. If the EC material is soluble in CH_3CN, EC performances of the device will be greatly affected (Bera et al., 2020). Hence, Fe-CP(5)-OAc is a promising candidate to fabricate EC film and devices.

The Effect of Structure on EC Performances

The assembled CPs film based on pyridine-bipyridine with different bond order complexes and the same ion (II) can deliver different colors and electrochemical cycling stability. Boom et al. illustrated the EC performances (optical modulation and cycling stability) can be adjusted by regulating the number of pyridine moieties and the pyridine-bipyridine bond order (H_2C-CH_2, HC = CH, C≡C) (Shankar et al., 2015). Bipyridine-based CP was also obtained by alternating deposition $PdCl_2$ and pyridine-based monomolecular. Both Fe-CP(1) and Fe-CP(2) show larger optical modulation compared to that of the Fe-CP(3) and Fe-CP(4). Fe-CP(2) film exhibits superior electrochemical stability with 30,000 cycles, which is attributed to the conjugated structure of L2 facilitating carrier transportation. Hiroshi et al. fabricated submicron-thick three-fold symmetric iron (II)-terpyridine (tpy) (Fe-CP(6)-BF_4, Fe-CP(7)-BF_4) nanosheets using a mild liquid-liquid synthesis (Takada et al., 2015). Compared with Fe-CP(6)-BF_4, the Fe^{3+}/Fe^{2+} redox couple of Fe-CP(7)-BF_4 shifted to a negative direction due to the strong electron-withdrawing ability of ethynylene linker. Furthermore, the MLCT band of Fe-CP(7)-BF_4 (588 nm) exhibits a slight bathochromic shift by 10 nm due to the ligands with electron withdrawing groups leading to an increase of electron cloud density. Nevertheless, the non-conjugated structure of the ligand could lead to the degradation of stability. In addition, they further successfully designed and synthesized Co(II) complex nanosheets with branched tris(terpyridine)-based ligand (L6) (Takada et al., 2015) or two triphenylamine-based branched tris(terpyridine) ligands (L8, L9) (Liu et al., 2019). The Co^{3+}/Co^{2+} and Co^{2+}/Co^{+} redox peaks were located at around -0.14 and -1.15 V *vs* Fc^{+}/Fc (Fc: ferrocene) for $[Co(tpy)_2]^{2+}$ unit of Co-CP(6)-BF_4, respectively (**Figures 3A,B**). The peak current of Co^{3+}/Co^{2+} was much smaller than Co^{2+}/Co^{+}, which is attributed to the slower electron transfer of Co^{3+}/Co^{2+} (Takada et al., 2015). Therefore, the color of film changed from orange to deep purple due to the redox couple of Co^{2+}/Co^{+} (**Figure 3C**). In addition, the oxidation potential of TPA/TPA (TPA:

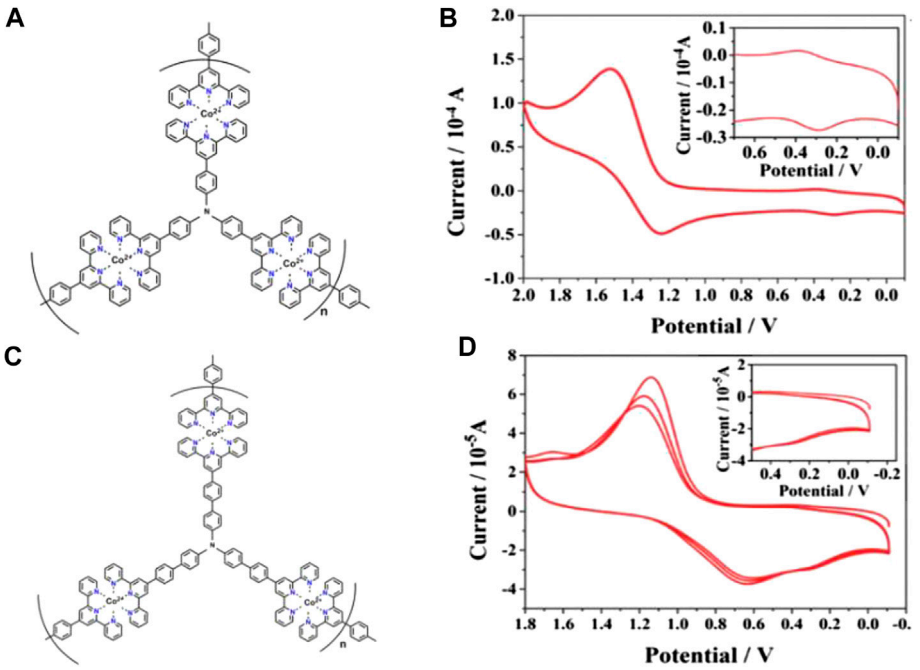

FIGURE 4 | The structure of **(A)** Co-CP(8)-BF_4 and **(C)** Co-CP(9)-BF_4. The CV of **(B)** Co-CP(8)-BF_4 and **(D)** Co-CP(9)-BF_4 in 1 M dichloromethane solution of $TBAPF_6$ with the scan speed of 0.1 V s^{-1}. Adapted with permission (Liu et al., 2019). Copyright 2019, Royal Society of Chemistry.

triphenylamine) in Co-CP(9)-BF_4 (**Figure 4C**) is higher than that of the Co-CP(8)-BF_4 (**Figure 4A**) because L9 possesses a stronger conjugation and electron delocalization relative to L8 (the inset in **Figures 4B,D**). Moreover, the amount of injected charge carriers exceeds the extracted charge carriers in the cyclic voltammetry (CV) graph (**Figure 4**), which may result in an unsatisfactory stability with 100 cycles (Liu et al., 2019). In conclusion, the structure of CPs has a great influence on the EC performances. We can optimize the EC performance by regulating the structure of CPs; for example, the optical properties would change by introducing electron-donating or electron-withdrawing groups into the ligand. And the study of the structure-property relationship will provide guidance for the furtherment of the field.

EC materials with the ability to switch more than two colored states can provide ample color variations for multicolor display. Till now, two primary strategies have been employed to develop organic multicolor EC polymers. One is to coordinate the same ligand with different metal ions. In order to verify this theory, a multicolor ECD was fabricated using Ru(II)/Fe(II)-based CP (Ru/Fe-CP(5)) as the EC layer and Prussian blue as the ion storage layer (Hsiao et al., 2019). The redox reactions of Fe^{2+}/Fe^{3+} and Ru^{2+}/Ru^{3+}occurred at 0.77/0.70 V and 0.93/0.84 V (*vs.* Ag/Ag^{+}), respectively (**Figure 5A**). During oxidation, the color changes from initial purple to orange, and then to light green (**Figure 5C**), which is attributed to the oxidation of Fe(II)Ru(II)-CP to Fe(III) Ru(II)-CP and finally formed to Fe(III)Ru(III)-CP and vice versa (Hsiao et al., 2019; Bera et al., 2019). The strength of the coordination bond determines the structural stability of CP during the EC reaction. For instance, the order of complexation strength between the metal ion and the same ligand is $Os^{2+} \geq Ru^{2+} > Fe^{2+} > Co^{2+}$, and the reaction is irreversible once it occurs (Xie et al., 2014). Based on this theory, Higuchi's group further precisely synthesized Fe(II)/Os(II)-based bimetallic CP (**Figure 6**).(Bera et al., 2020; Bera et al., 2019) The Fe(II)/Os(II)-CP(5)-OAc ECD exhibits multicolor changes upon the applied potential range from 0.0 to 1.0 V (*vs.* Ag/Ag^{+}) with an optical modulation of 52% at 575 nm. Another strategy is to synthesize EC materials that combined other colored units into a terpyridine-based line. Zhang et al. employed a three-arm molecule "tris [4-(4′-2,2′: 6′,2″-terpyridyl)-phenyl]amine (L8)" (TPA-YPY) with triphenylamine located in the central core connected with terpyridine as the peripheral arms to coordinate with ion (II), constructing a multicolor Fe-CP(8) EC material (**Figure 4A**). (Kuai et al., 2019) The CV curve shows two obvious reversible redox couples, located at 1.35/0.97 V and 1.49/1.27 V *vs.* Ag/AgCl, corresponding to the redox behaviors of the coordinated Fe(II)-terpyridine unit and the central triphenylamine group, respectively (**Figure 7A**). The color of film changes from red to orange along with the elevation of the potential from 0 to 1.4 V, accompanying the intensity of the absorption peak at 580 nm decreasing till it disappears and the intensity of absorption peak at 421 nm increasing obviously due to the oxidation of Fe(II)-terpyridine group. When the applied potential was further increased to 1.6 V (vs. Ag/AgCl), a new peak emerged at 780 nm together with the color change to green. Obviously, the redox-active Fe-CP(8) exhibits a color variation from magenta to orange and then to green by the two redox processes of Fe(II)-pyridine and triphenyl ammonium groups, respectively (**Figure 7B**). The fabricated ECD shows a similar EC

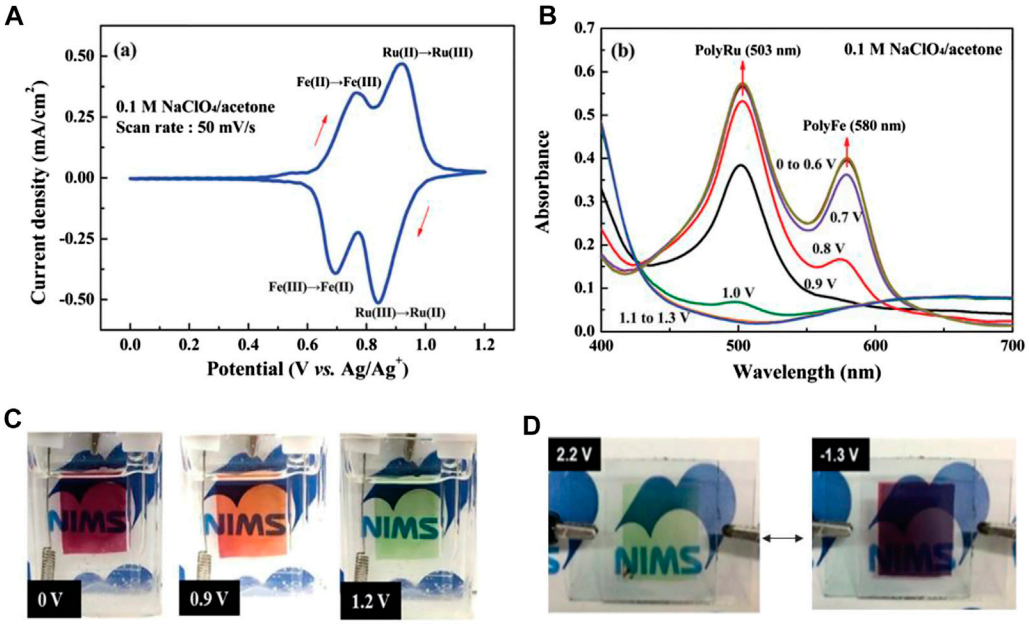

FIGURE 5 | (A) CV of the RuFe-CP film in 0.1 M $NaClO_4/CH_3CN$. **(B)** UV-Vis spectra of the PolyRuFe film at potential range between 0 and 1.2 V (*vs*. Ag/Ag^+). **(C)** *In situ* digital photograph of RuFe-CP at bleached state and colored state. **(D)** Images of the RuFe-CP based ECD at the bleached (2.2 V *vs*. Ag/Ag^+) and colored (-1.3 V *vs*. Ag/Ag^+) states. Adapted with permission (Hsiao et al., 2019). Copyright 2019, American Chemical Society.

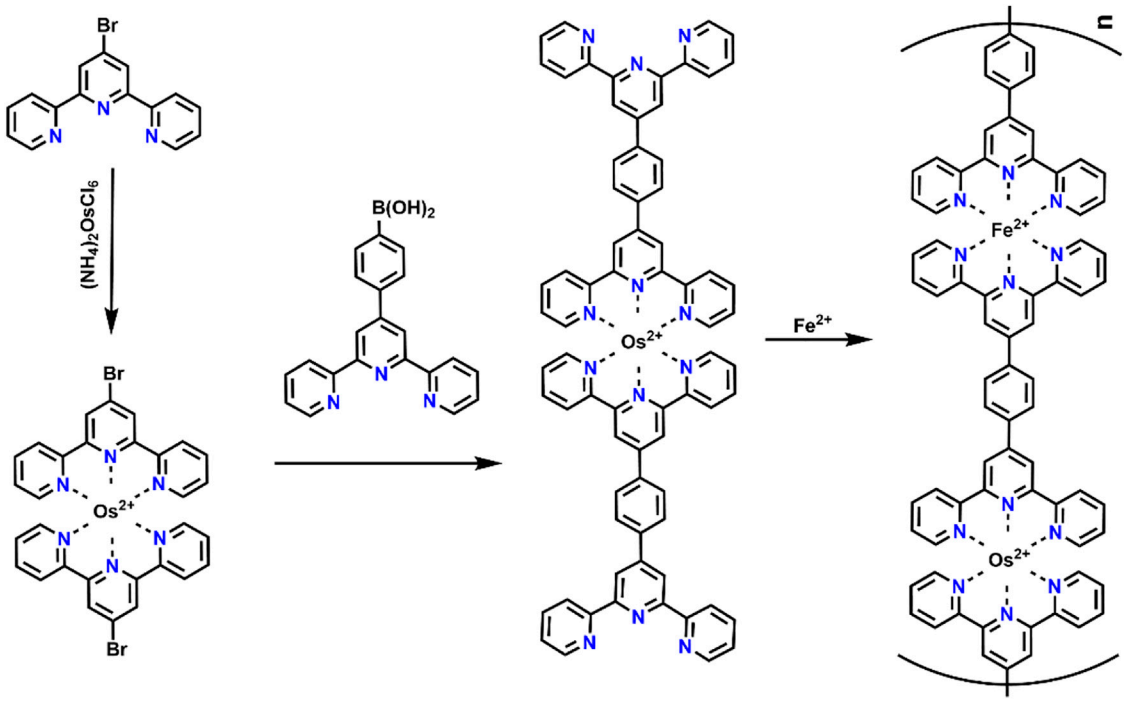

FIGURE 6 | Schematic representation of the preparation of Fe/Os-CP.

performance to thin films (**Figures 7C–E**). In brief, molecular design strategy provides a new and effective way for the preparation of multicolor materials. Moreover, the development of multicolor ECDs would meet the requirements of different application areas. Multicolor ECDs are easily realized by assembling two electrode-coating EC materials in one cell, and

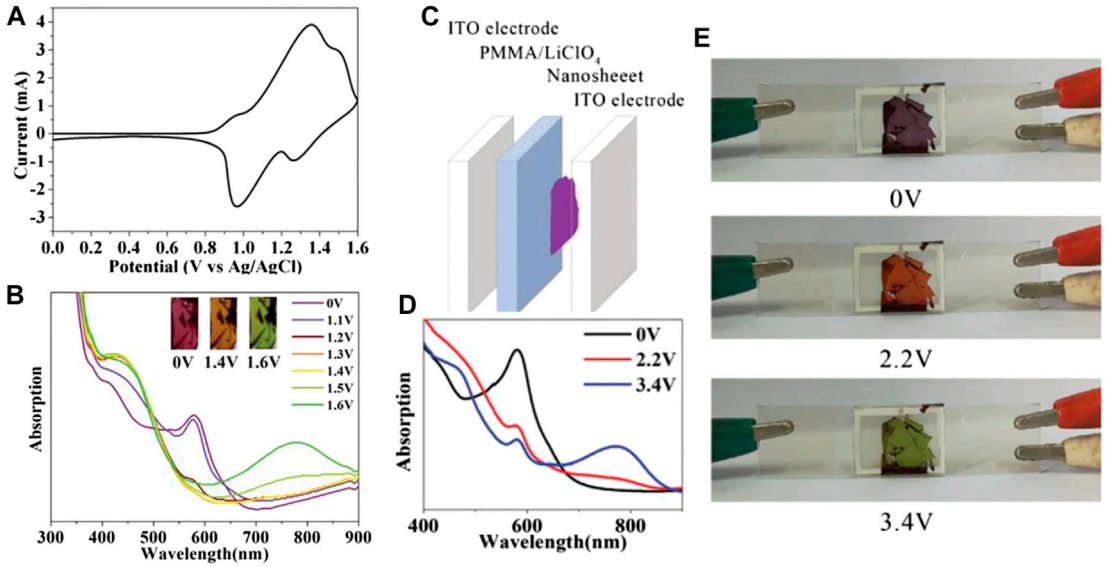

FIGURE 7 | (A) CV of the Co-CP(8) nanosheet. **(B)** UV-vis spectra of the Co-CP(8) nanosheet at potential from 0 to 1.6 V *vs* Ag/AgCl in a solution of 0.1 M Bu_4NClO_4/CH_3CN (Inset: The color of Co-CP(8) film corresponding to the applied different potentials.) **(C)** The structure of the solid-state device. **(D)** UV-vis spectrum of the solid-state device applied potential from 0 to 3.4 V *vs* Ag/AgCl. **(E)** The color of the solid-state device at 0 V *vs* Ag/AgCl, 2.2 V *vs* Ag/AgCl and 3.4 V *vs* Ag/AgCl. Adapted with permission (Kuai et al., 2019). Copyright 2019, Royal Society of Chemistry.

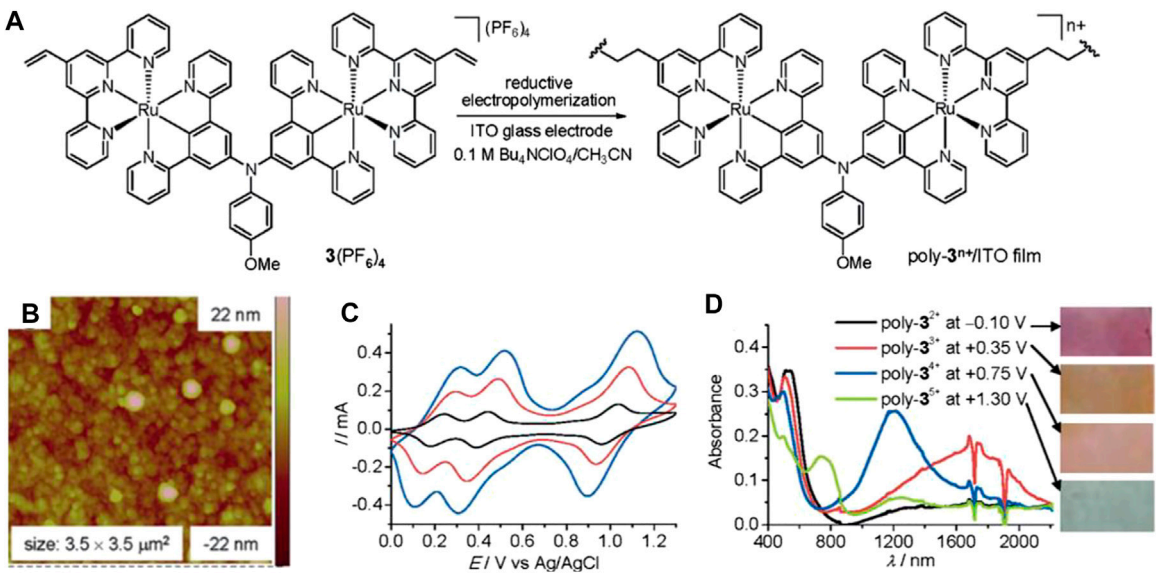

FIGURE 8 | (A) Demonstration for the reductive electropolymerization **(B)** AFM image of the obtained Ru-CP film. **(C)** CVs at100 mV s^{-1} of the Ru-CP film on ITO obtained at 15 (black line), 30 (red line), and 45 (blue line) electrochemistry cycles. **(D)** Absorption spectra and film picture of the Ru-CP film at different redox states. Adapted with permission (Cui et al., 2015). Copyright 2015, Wiley-VCH.

the color of the device could be regulated selectively via the applied voltage.

Optical memory is a distinct advantage of energy-efficient ECDs that do not require additional energy consumption to maintain the colored and bleached state after powering off. However, the conjugated structure of the ligand facilitates the transfer of ions and electrons, resulting in poor optical memory. Recently, Chakraborty and co-workers fabricated a non-conjugated 3tpy ligand to limit the electron transfer/hopping inside the EC film, which successfully enhanced the memory. It

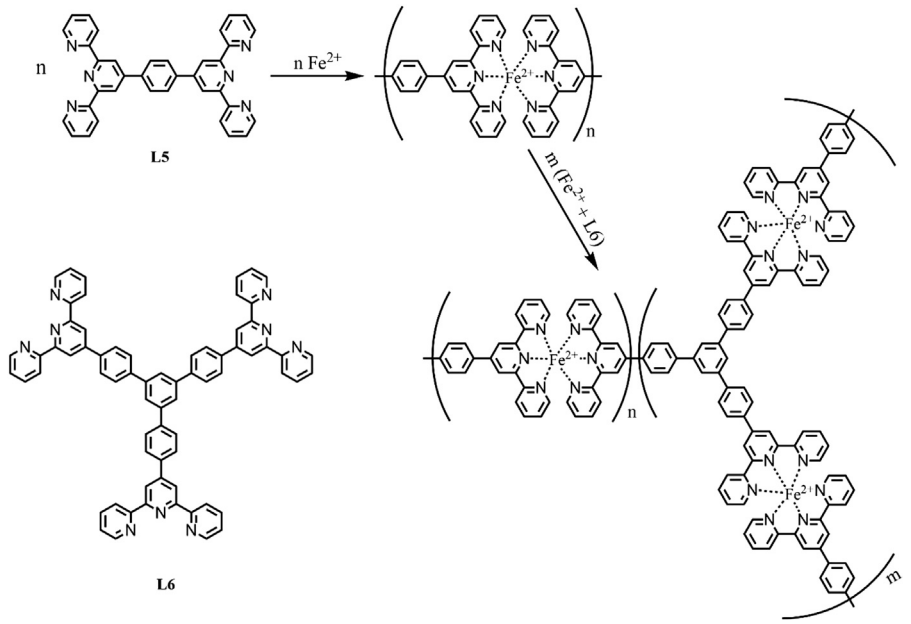

FIGURE 9 | Synthesis of the 3-D Fe-CP(L5 x% L6 y%).

can be seen that it provided 50% retention of the bleached state till 25 min after powering off (Roy and Chakraborty, 2020). Both colored speed (1.15 s) and bleached speed (2.49 s) are slightly slower than that of conjugated 3tpy ligand, which stem from the limitation of electron transfer by non-conjugated ligands.

The ECD with the function of near-infrared range modulation can effectively regulate the heat flux of the device. Based on the above function, applications of ECD can be extended to infrared dynamic display, camouflage, thermal regulation, and other fields. Lots of inorganic materials, i.e., NiO (Cai et al., 2014), WO_3 (Reddy et al., 2015), and so on, exhibit near-infrared EC properties, but few CPs have the ability to regulate near-infrared light. Recently, Zhong et al. prepared a Ru-CP film with a redox-active amine bridge using the electro-polymerization method (**Figure 8A**), (Cui et al., 2015a) which displays multistate NIR EC properties with low operational potential and good optical modulation. Moreover, the corresponding film successively displays four colors in different oxidation states (**Figure 8D**). (Cui et al., 2015a; Cui et al., 2015b) Park et al. recently synthesized an Fe-CP based on a line terpyridine-based ligand with phthalocyanine (Pc) as a spacer; it shows a color variation from blue to transparent green (Arockiam et al., 2019). Moreover, the Pc-based Fe-CPs have the ability to modulate light in the infrared region, which is mainly due to the presence of Pc spacer by delocalizing the charge throughout the CP. These studies will evoke intense interest in developing new EC materials for commercial applications.

Besides the species of the ligands and metal ions, the molecular structure of organic polymers, such as linear, hyperbranched, dendritic, and network, also have important effects on the electrochemical, electrochromic, and mechanical properties. Therefore, compared with the linear polymers, CP with a hyperbranched structure is expected to show excellent EC performance. For example, the three-dimensional structured Fe-CP showed a faster switching speed (colored time: 0.19 s, bleached time: 0.36 s) than that of the one dimensional linear polymer because the highly porous hyperbranched structure facilitates fast ion transport within the active materials (**Figure 9**). (Hu et al., 2014). However, the large holes and porous structure will disappear with increasing of the ratio of tris(terpyridine) ligand, resulting in poor EC performances. This phenomenon suggests that the porous microstructure is beneficial to obtaining high-performance EC films and devices.

Methods for Preparing Electrochromic Films

So far, extensive efforts have been made to develop facile and low-cost coating methods to fabricate high-quality and scalable EC films. Different film coating methods may lead to different morphologies, microstructures, and uniformity, which have a significant impact on the EC and electrochemical performances of ECDs. Therefore, it is of high importance to choose the appropriate film coating method for developing high-performance and large area ECDs in an economic way. The comparative analysis of different film coating methods is concluded and shown in **Table 1**. Up to now, the widespread EC film coating methods include spray coating, electrostatic spraying, electro-polymerization, chemical bath deposition (CBD), and inkjet printing. As an easy, economic, and high-efficiency solution-processing technology, spray coating is one

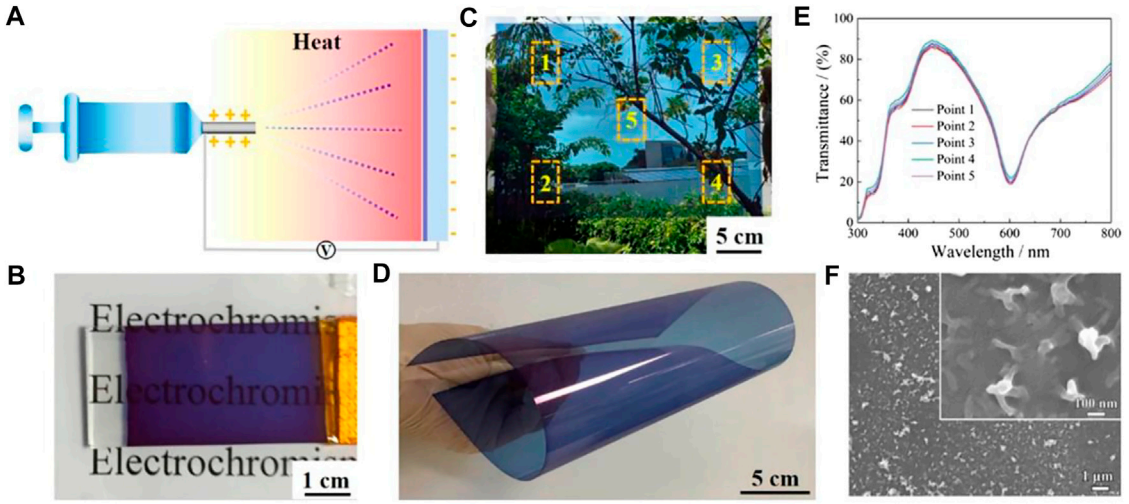

FIGURE 10 | (A) Representation of ESD strategy to fabricate Fe-CP(5) film **(B and C)** Digital photograph of Fe-CP(5) film on rigid/flexible substrate. **(D)** Bendable demonstration of flexible Fe-CP(5) film. **(E)** UV-vis spectra of the Fe-CP(5) film at five points. **(F)** SEM of Fe-CP(5) film. Adapted with permission (Cai et al., 2020a). Copyright 2020, American Chemical Society.

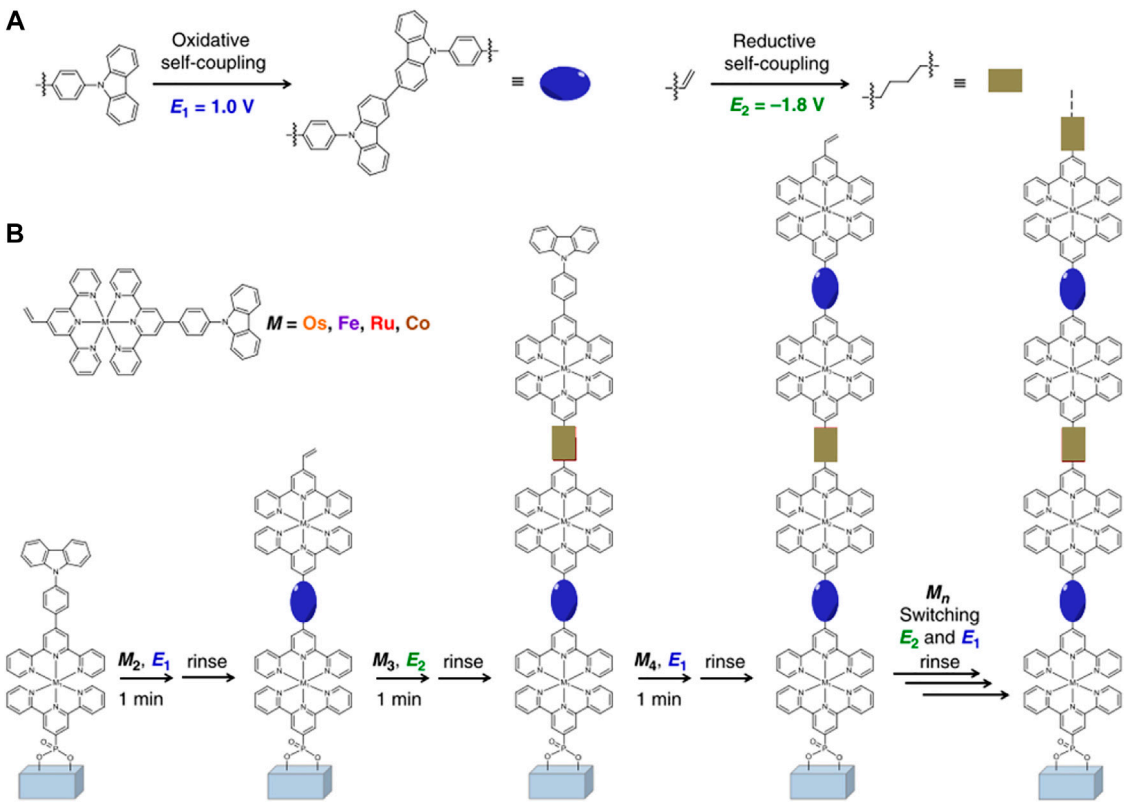

FIGURE 11 | Rapidly iterative electrodeposition of organometallic polymers at 1.0 V *vs*. Ag/Ag^+ and −1.8 V *vs*. Ag/Ag^+, respectively. Adapted with permission (Zhang J. et al., 2020). Copyright 2020, Nature Publishing Group.

of the most popular film coating methods. A semi-solid-state ECD can be constructed by assembling the spray coated Fe-CP(5) film onto ITO/glass. The obtained semi-solid-state ECD exhibits long-term durability and fast switching speed. The optical modulation remains at 95% after 1,000 cycles, indicating excellent cycling stability (Mondal et al., 2019c; Mondal et al., 2019d).

TABLE 1 | comparison of coating films highlighting advantages and disadvantages.

	Reference	Advantage	Disadvantage
Spraying coating	Mondal et al. (2019c, 2019d)	Simple and convenient	Weak adhesion
Electro-polymerization	Zhang J. et al. (2020)	Precisely controllable molecular weight	System limitations
Chemical bath deposition	Cai et al. (2020b)	Facile and scalable	High waste
Inkjet printing	Chen et al. (2015)	Pattern, large area, and easy industrialization	Need high-quality ink

Nevertheless, the chief drawback of the spray coating method is that it is hard to control the uniformity of the film thickness on a large scale, and it is also accompanied by weak adhesion between the active film and the substrate. Electrostatic spraying technology is a simple, accurate, and scalable film coating approach which can be used to fabricate large area EC films with controllable morphology (Ju et al., 2014; Xu et al., 2019). During the film coating process, electroactive materials can be directly deposited on conductive substrates under the electrostatic attraction during the coating process. Using the electrostatic spraying technique, Cai and co-workers fabricated large-area Fe-CP(5)-OAc film onto both FTO/glass and ITO/PET substrates (**Figure 10**). (Cai et al., 2020) ECD based on Fe-CP(5)-OAc achieved an ultrahigh coloration efficiency (750.3 cm^2 C^{-1}) and a robust electrochemical stability with 10,000 cycles. Moreover, functionalized CPs were prepared by *in situ* electro-polymerization and deposition without any additive simultaneously. Li et al. developed a bottom-up electro-polymerization method to fabricate uniform and sequence-controlled CPs films by accurately inserting C-C couplings of distinct monomers (**Figure 11**) (Zhang J. et al., 2020). This sequence-controlled electro-polymerization offered an accurate way to quantitatively analyze the structure-performance relationship of the EC materials. The molecular structures and degree of polymerization of a definite product can be precisely controlled. However, the film prepared by the above-mentioned methods requires 'tailoring' to obtain a complicated pattern, which may result in the waste of active materials. Inkjet printing, as a precise and direct digital film coating technology, has been emerging for preparation of high-quality EC film recently. This printing technology presents many advantages, such as high-resolution patterns, efficient use of materials, and applicability for a variety of substrates. Liao and coworkers fabricated a flexible EC film on a flexible ITO-polyethylene-naphthalate (PEN) substrate via inkjet-printed mixed Ru-CP and Fe-CP inks (Chen et al., 2015). By accurately adjusting the print dosages of each EC material, the color of the obtained EC film can be controlled directly without premixing materials. The flexible ECD using Ru-CP and Fe-CP possessed high coloration efficiency (445 cm^2 C^{-1}) and fast switching speed at both bendable and origin states. Therefore, the preparation method of thin films influences the microtopography, which in turn affects the EC performances and their commercial price. Developing ECDs with low cost, high performances, and a large-scale manufacturing method will promote rapid commercialization of this field. Electrostatic spraying will be a promising fabrication method due to its controllable morphologic and strong binding force between substrate and materials.

Electrochromic and Multifunctional Devices

The multifunctional ECD which combines EC technology with other technologies, such as flexible, stretchable, energy storage, display, and sensing technologies, has received considerable attention recently. Moreover, the device with functions of EC and energy storage have been investigated extensively. Cai et al. reported a 1-dimensional π-d conjugated CP composed of metal ion (Ni^{2+}) and organic linker (1,2,4,5-benzenetetramine (BTA)) (Cai et al., 2020b). This material can be directly grown on a transparent FTO substrate. In particular, the Ni-BTA nanowire film can maintain its electrochemical charge-discharge capacity and EC performance after 10,000 electrochemical cycles, verifying its excellent durability. Interestingly, energy-storage ECD can be constructed as an intelligent energy-storage indicator to detect the electric energy level through color. It is a unique perspective to estimate the states of energy-storage. The excellent EC properties and charge storage properties of Ni-BTA nanowire films provide a broad application prospect as electrode materials in EC devices, energy storage batteries, and multifunctional smart windows. In order to enrich its characteristics and expand its application range, more and more attention should be paid to the integration of ECDs with other functions. With the development of flexible transparent electrodes, wearable devices become the darling of the next generation of electronic devices. Novel ECDs with integration of EC technology with flexible and wearable technology have great potential for use in prospective smart clothes and implantable displays.

CONCLUSIONS AND OUTLOOK

CPs with the advantages of low cost, light weight, and flexibility have broad application prospects in energy efficient fields. This review has summarized various functional EC materials and devices fabricated via the supramolecular strategy based on metal-ligand coordination. Although great progress in experimental aspects has been achieved, some issues still need to be addressed. As we know, the key to the EC process is redox reaction, which is accompanied by the ion and electron injection/extraction process. However, current research mainly focuses on either the electron transport process or the ion diffusion process. Theoretically, simultaneously improving the electron and ion insertion/extraction process can effectively promote EC performances. Additionally, the detail process of the electron and ion transport would be further revealed by virtue of the

combination of *in situ* and theoretical modeling, which will in turn provide effective guides for better molecular design and device fabrication. Further, benefiting from the development of flexible conductive substrate, the soft and flexible devices are fabricated. The same prototype devices are only realized under laboratory conditions. However, it is still a huge challenge to prepare large-area high-quality ECDs for practical application. At present, although EC technology has been used in high-end cars and Boeing 787 Dreamliner smart windows as well as smart phone shells, it is still a great challenge to utilize ECDs in our daily life. Therefore, the development of low-cost and high-performance ECDs shows great potential for the application of ECDs in the future.

In summary, CPs provide a promising approach for the development of functional materials in the EC field. However, in order to improve the optoelectronic performance of ECDs, more efforts are still necessary to design new CP molecules and microstructures. We believe this review will inspire more research on the development of functional CPs materials for EC in the future.

AUTHOR CONTRIBUTION

GC proposed the research direction and guided the project. SL and CW were the primary writers of the manuscript. PZ and JF revised the article language. All authors discussed the results and provided feedback on the manuscript.

FUNDING

This work was financially supported by the National Natural Science Foundation of China (U2004175, 51902086).

REFERENCES

Arockiam, J. B., Son, H., Han, S. H., Balamurugan, G., Kim, Y. H., and Park, J. S. (2019). Iron phthalocyanine incorporated metallo-supramolecular polymer for superior electrochromic performance with high coloration efficiency and switching stability. *ACS Appl. Energ. Mater.* 2, 8416–8424. doi:10.1021/acsaem.9b01022

Bera, M. K., Ninomiya, Y., and Higuchi, M. (2020). Constructing alternated heterobimetallic Fe(II)/Os(II) supramolecular polymers with diverse solubility for facile fabrication of voltage-tunable multicolor electrochromic devices. *ACS Appl. Mater. Interfamces* 12, 14376–14385. doi:10.1021/acsami.9b21966

Bera, M. K., Ninomiya, Y., Yoshida, T., and Higuchi, M. (2019). Precise synthesis of alternate Fe(II)/Os(II)-Based bimetallic metallo-supramolecular polymer. *Macromol. Rapid Comm.* 41, 1900384. doi:10.1002/marc.201900384

Cai, G. F., Chen, J., Xiong, J., Eh, A. L., Wang, J., Higuchi, M., et al. (2020a). Molecular level assembly for high-performance flexible electrochromic energy-storage devices. *ACS Energ. Lett.* 5, 1159–1166. doi:10.1021/acsenergylett.0c00245

Cai, G. F., Cui, M., Kumar, V., Darmawan, P., Wang, J., Wang, X., et al. (2016b). Ultra-large optical modulation of electrochromic porous WO_3 film and the local monitoring of redox activity. *Chem. Sci.* 7, 1373–1382. doi:10.1039/c5sc03727a

Cai, G. F., Cui, P., Shi, W., Morris, S., Lou, Sh. N., et al. (2020b). One-dimensional π-d conjugated coordination polymer for electrochromic energy storage device with exceptionally high performance. *Adv. Sci.* 7, 1903109. doi:10.1002/advs.201903109

Cai, G. F., Darmawan, P., Cheng, X., and Lee, P. S. (2017). Inkjet printed large area multifunctional smart windows. *Adv. Energ. Mater.* 7, 1602598. doi:10.1002/aenm.201602598

Cai, G. F., Darmawan, P., Cui, M., Wang, J., Chen, J., Magdassi, S., et al. (2016a). Highly stable transparent conductive silver grid/PEDOT:PSS electrodes for integrated bifunctional flexible electrochromic supercapacitors. *Adv. Energ. Mater.* 6, 1501882. doi:10.1002/aenm.201501882

Cai, G. F., Tu, J., Zhou, D., Zhang, J., Xiong, Q., Zhao, X., et al. (2013). Multicolor electrochromic film based on TiO_2@Polyaniline core/shell nanorod array. *J. Phys. Chem. C* 117, 15967–15975. doi:10.1021/jp4056939

Cai, G. F., Wang, X., Cui, M., Darmawan, P., Wang, J. X., Eh, A. L., et al. (2014). Electrochromo-supercapacitor based on direct growth of NiO nanoparticles. *Nano Energy* 12, 258–267.

Chen, B.-H., Kao, S.-Y., Hu, C.-W., Higuchi, M., Ho, K.-C., and Liao, Y.-C. (2015). Printed multicolor high-contrast electrochromic devices. *Acs Appl. Mater. Inter.* 7, 25069–2507676. doi:10.1021/acsami.5b08061

Christiansen, D. T., Tomlinson, A. L., and Reynolds, J. R. (2019). New design paradigm for color control in anodically coloring electrochromic molecules. *J. Am. Chem. Soc.* 141, 3859–3862. doi:10.1021/jacs.9b01507

Cui, B. B., Tang, J. H., Yao, J., and Zhong, Y. W. (2015a). A molecular platform for multistate near-infrared electrochromism and flip-flop, flip-flap-flop, and ternary memory. *Angew. Chem. Int.l* 54, 9324–9329. doi:10.1002/anie.201504584

Cui, B. B., Zhong, Y. W., and Yao, J. (2015b). Three-state near-infrared electrochromism at the molecular scale. *J. Am. Chem. Soc.* 137, 4058–4061. doi:10.1021/jacs.5b00586

Deb, S. K. (2006). Optical and photoelectric properties and colour centres in thin films of tungsten oxide. *Philos. Mag.* 27, 801–822. doi:10.1080/14786437308227562

Dey, K., Pal, M., Rout, K. C., Kunjattu, H. S., Das, A., Mukherjee, R., et al. (2017). Selective molecular separation by interfacially crystallized covalent organic framework thin films. *J. Am. Chem. Soc.* 139, 13083–13091. doi:10.1021/jacs.7b06640

Duan, J., Li, Y., Pan, Y., Behera, N., and Jin, W. (2019). Metal-organic framework nanosheets: an emerging family of multifunctional 2D materials. *Coordin. Chem. Rev.* 395, 25–45. doi:10.1016/j.ccr.2019.05.018

Fan, C., Ye, C., Wang, X., Chen, Z., Zhou, Y., Liang, Z., et al. (2015). Synthesis and electrochromic properties of new terpyridine-triphenylamine hybrid polymers. *Macromolecules* 48, 6465–6473. doi:10.1021/acs.macromol.5b00493

Feng, J. F., Liu, T. F., and Cao, R. (2020). An electrochromic hydrogen-bonded organic framework film. *Angew. Chem. Int. Ed.* 59, 22392–22396. doi:10.1002/anie.202006926

Higuchi, M. (2014). Stimuli-responsive metallo-supramolecular polymer films: design, synthesis and device fabrication. *J. Mater. Chem. C* 2, 9331–9341. doi:10.1039/c4tc00689e

Hsiao, L. Y., Chang, T. H., Lu, H. C., Wang, Y. C., Lu, Y. A., Ho, K. C., et al. (2019). A panchromatic electrochromic device composed of Ru(II)/Fe(II)-based heterometallo-supramolecular polymer. *J. Mater. Chem. C* 7, 7554–7562. doi:10.1039/c9tc01452g

Hsu, C. Y., Zhang, J., Moriyama, S., and Higuchi, M. (2016). Solvent effect on electrochemical properties of a Co(II)-Based metallo-supramolecular polymer film. *Macromol. Symp.* 363, 12–19. doi:10.1002/masy.201500136

Hu, C. W., Sato, T., Zhang, J., Moriyama, S., and Higuchi, M. (2013). Multi-colour electrochromic properties of Fe(II)/Ru(II)-based bimetallo-supramolecular polymers. *J. Mater. Chem. C* 1, 3408–3413. doi:10.1039/c3tc30440j

Hu, C. W., Sato, T., Zhang, J., Moriyama, S., and Higuchi, M. (2014). Three-dimensional Fe(II)-based metallo-supramolecular polymers with electrochromic properties of quick switching, large contrast, and high coloration efficiency. *ACS Appl. Mater. Inter.* 6, 9118–9125. doi:10.1021/am5010859

Huang, H. B., Yu, K., Zhang, N., Xu, J. Y., Yu, X. T., Liu, H. X., et al. (2020). Localized surface plasmon resonance enhanced visible-light-driven CO_2 photoreduction in Cu nanoparticl loaded ZnInS solid solutions. *Nanoscale* 12, 15169–15174. doi:10.1039/d0nr01801e

Ju, M. J., Jeon, I.-Y., Lim, K., Kim, J. C., Choi, H.-J., Choi, I. T., et al. (2014). Edge-carboxylated graphene nanoplatelets as oxygen-rich metal-free cathodes for organic dye-sensitized solar cells. *Energy Environ. Sci.* 7, 1044–1052. doi:10.1039/c3ee43732a

Keum, K., Kim, J. W., Hong, S. Y., Son, J. G., Lee, S. S., and Ha, J. S. (2020). Flexible/stretchable supercapacitors with novel functionality for wearable electronics. *Adv. Mater.* 32, 2002180. doi:10.1002/adma.202002180

Kuai, Y., Li, W., Dong, Y., Wong, W. Y., Yan, S., Daia, Y., et al. (2019). Multi-color electrochromism from coordination nanosheets based on a terpyridine-Fe(II) complex. *Dalton T* 48, 15121–15126. doi:10.1039/c9dt02980j

Kung, C. W., Wang, T. C., Mondloch, J. E., Jimenez, D. F., Gardner, D. M., Bury, W., et al. (2013). Metal-organic framework thin films composed of free-standing acicular nanorods exhibiting reversible electrochromism. *Chem. Mater.* 25, 5012–5017. doi:10.1021/cm403726v

Lahav, M., and van der Boom, M. E. (2018). Polypyridyl metallo-organic assemblies for electrochromic applications. *Adv. Mater.* 30, 1706641. doi:10.1002/adma.201706641

Lang, A. W., Österholm, A. M., and Reynolds, J. R. (2019). Paper-based electrochromic devices enabled by nanocellulose-coated substrates. *Adv. Funct. Mater.* 29, 1903487. doi:10.1002/adfm.201903487

Leem, G., Keinan, S., Jiang, J., Chen, Z., Pho, T., Morseth, Z. A., et al. (2015). $Ru(bpy)_3^{2+}$ derivatized polystyrenes constructed by nitroxide-mediated radical polymerization. Relationship between polymer chain length, structure and photophysical properties. *Polym. Chem.* 6, 8184–8193. doi:10.1039/c5py01289a

Li, M.He, Q., Li, Z., Li, Q., Zhang, Y., Meng, J., et al. (2019). A novel dendrite-free Mn^{2+}/Zn^{2+} hybrid battery with 2.3 V voltage window and 11000-cycle lifespan. *Adv. Energ. Mater.* 9, 1901469. doi:10.1002/aenm.201901469

Li, X.Perera, K., He, J., Gumyusenge, A., and Mei, J. (2019). Solution-processable electrochromic materials and devices: roadblocks and strategies towards large-scale Applications. *J. Mater. Chem. C* 7, 12761–12789. doi:10.1039/c9tc02861g

Li, X., Wei, J., Li, Q., Zheng, S., Xu, Y., Du, P., et al. (2018). Nitrogen-Doped cobalt oxide nanostructures derived from cobalt-alanine complexes for high-performance oxygen evolution reactions. *Adv. Funct. Mater.* 28, 1800886. doi:10.1002/adfm.201800886

Liu, Y., Sakamoto, R., Ho, C. L., Nishihara, H., and Wong, W. Y. (2019). Electrochromic triphenylamine-based cobalt (II) complex nanosheets. *J. Mater. Chem. C* 7, 9159–9166. doi:10.1039/c9tc02257k

Madasamy, K., Velayutham, D., Suryanarayanan, V., Kathiresan, M., and Ho, K. C. (2019). Viologen-based Electrochromic materials and devices. *J. Mater. Chem. C* 7, 4622–4637. doi:10.1039/c9tc00416e

Mondal, S., Ninomiya, Y., Yoshida, T., Mori, T., Bera, M. K., Ariga, K., et al. (2020b). Dual-branched dense hexagonal Fe(II)-Based coordination nanosheets with red-to-colorless electrochromism and the durable device fabrication. *ACS Appl. Mater. Inter.* 12, 31896–31903. doi:10.1021/acsami.0c05921

Mondal, S., Yoshida, T., and Higuchi, M. (2019c). Electrochromic devices using Fe(II)-based metallo-supramolecular polymer: introduction of ionic liquid as electrolyte to enhance the thermal stability. *J. Soc. Inf. Display* 27, 1–6. doi:10.1002/jsid.833

Mondal, S., Yoshida, T., Maji, S., Ariga, K., and Higuchi, M. (2020a). Transparent supercapacitor display with redox-active metallo-supramolecular polymer films. *ACS Appl. Mater. Inter.* 12, 16342–16349. doi:10.1021/acsami.9b23123

Mondal, S., Yoshida, T., Rana, U., Bera, M. K., and Higuchi, M. (2019d). Thermally stable electrochromic devices using Fe(II)-based metallo-supramolecular polymer. *Sol. Energ. Mater Sol. Cell* 200, 110000. doi:10.1016/j.solmat.2019.110000

Muronoi, Y., Zhang, J., Higuchi, M., and Maki, H. (2013). Electrochemical switching of luminescence in Ru(II)-based metallosupramolecular polymer device. *Chem. Lett.* 42, 761–763. doi:10.1246/cl.130158

Ninomiya, Y., Yoshida, T., and Higuchi, M. (2020). Electrochromic Fe(II)-based metallo-supramolecular polymers: color modulation by spacer modification in bisterpyridine ligand. *Chem. Lett.* 49, 1003–1005. doi:10.1246/cl.200307

Reddy, B. N., Kumar, P. N., and Deepa, M. (2015). A poly(3,4-ethylenedioxypyrrole)-Au@WO_3-based electrochromic pseudocapacitor. *Chemphyschem* 16, 377–389. doi:10.1002/cphc.201402625

Roy, S., and Chakraborty, C. (2020). Interfacial coordination nanosheet based on non-conjugated three-arm terpyridine: a highly color-efficient electrochromic material to converge fast switching with long optical memory. *ACS Appl. Mater. Inter.* 12, 35181–35192. doi:10.1021/acsami.0c06045

Rubio-Gimenez, V., Galbiati, M., Castells-Gil, J., Almora-Barrios, N., Navarro-Sanchez, J., Escorcia-Ariza, G., et al. (2018). Bottom-up fabrication of semiconductive metal-organic framework ultrathin films. *Adv. Mater.* 30, 1704291. doi:10.1002/adma.201704291

Savagian, L. R., Osterholm, A. M., Shen, D. E., Christiansen, D. T., Kuepfert, M., and Reynolds, J. R. (2018). Conjugated polymer blends for high contrast black-to-transmissive electrochromism. *Adv. Opt. Mater.* 6, 1800594. doi:10.1002/adom.201800594

Shankar, S., Lahav, M., and van der Boom, M. E. (2015). Coordination-based molecular assemblies as electrochromic materials: ultra-high switching stability and coloration efficiencies. *J. Am. Chem. Soc.* 137, 4050–4053. doi:10.1021/jacs.5b00429

Somani, P. R., and Radhakrishnan, S. (2002). Electrochromic materials and devices present and future. *Mater. Chem. Phys.* 77, 117–133.

Takada, K., Sakamoto, R., Yi, S. T., Katagiri, S., Kambe, T., and Nishihara, H. (2015). Electrochromic bis(terpyridine)metal complex nanosheets. *J. Am. Chem. Soc.* 137, 4681–4689. doi:10.1021/ja510788b

Tian, Y., Cong, S., Su, W., Chen, H., Li, Q., Geng, F., et al. (2014). Synergy of $W_{18}O_{49}$ and polyaniline for smart supercapacitor electrode integrated with energy level indicating functionality. *Nano Lett.* 14, 2150–2156. doi:10.1021/nl5004448

Wang, S., Gao, W., Hu, X. Y., Shen, Y. Z., and Wang, L. (2019c). Supramolecular strategy for smart windows. *Chem. Commun.* 55, 4137–4149. doi:10.1039/c9cc00273a

Wang, Y., Wang, S., Wang, X., Zhang, W., Zheng, W., Zhang, Y. M., et al. (2019b). A multicolour bistable electronic shelf label based on intramolecular proton-coupled electron transfer. *Nat. Mater.* 18, 1335–1342. doi:10.1038/s41563-019-0471-8

Wang, Y. Y., Ban, Y. L., Nie, Z., and Sim, C. Y. D. (2019a). Dual-loop antenna for 4G LTE MIMO smart glasses applications. *IEEE Antenn. Wirel. Pr.* 18, 1818–1822. doi:10.1109/lawp.2019.2930726

Wałęsa-Chorab, M., Banasz, R., Marcinkowski, D., Kubicki, M., and Patroniak, V. (2017). Electrochromism and electrochemical properties of complexes of transition metal ions with benzimidazole-based ligand. *RSC Adv.* 7, 50858–50867.

Xie, T. Z., Liao, S. Y., Guo, K., Lu, X., Dong, X., Huang, M., et al. (2014). Construction of a highly symmetric nanosphere via a one-pot reaction of a tristerpyridine ligand with Ru(II). *J. Am. Chem. Soc.* 136, 8165–8168. doi:10.1021/ja502962j

Xu, Q., Pang, H., Xue, H., Li, Q., and Zheng, S. (2020). A highly alkaline-stable metal oxide@metal–organic framework composite for high-performance electrochemical energy storage. *Natl. Sci. Rev.* 7, 305–314. doi:10.1093/nsr/nwz137

Xu, S., Lv, C., He, T., Huang, Z., and Zhang, C. (2019). Amorphous film of cerium doped cobalt oxide as a highly efficient electrocatalyst for oxygen evolution reaction. *J. Mater. Chem. A.* 7, 7526–7532. doi:10.1039/c9ta00061e

Yen, H. J., and Liou, G. S. (2018). Recent advances in triphenylamine-based electrochromic derivatives and polymers. *Polym. Chem.* 9, 3001–3018. doi:10.1039/c8py00367j

Zhang, J.Wang, J., Wei, C., Wang, Y., Xie, G., Li, Y., et al. (2020). Rapidly sequence-controlled electrosynthesis of organometallic polymers. *Nat. Commun.* 11, 2530. doi:10.1038/s41467-020-16255-z

Zhang, T.Zhang, L., Zhao, L., Huang, X., and Hou, Y. (2020). Catalytic effects in the cathode of Li-S batteries: accelerating polysulfides redox conversion. *EnergyChem.* 2, 100036. doi:10.1016/j.enchem.2020.100036

Zhang, W., Wang, X., Wang, Y., Yang, G., Gu, C., Zheng, W., et al. (2019). Bio-inspired ultra-high energy efficiency bistable electronic billboard and reader. *Nat. Commun.* 10, 1559. doi:10.1038/s41467-019-09556-5

Zhou, Y., Wang, S., Peng, J., Tan, Y., Li, C., Boey, F. Y. C., et al. (2020). Liquid thermo-responsive smart window derived from hydrogel. *Joule* 4, 1–17. doi:10.1016/j.joule.2020.09.001

Conflict of Interest: The authors declare that the research was conducted in the absence of any commercial or financial relationships that could be construed as a potential conflict of interest.